Progressive coding for hyperspectral signature characterization

Chein-I Chang, FELLOW SPIE
University of Maryland Baltimore County
Department of Computer Science and Electrical Engineering
Remote Sensing Signal and Image Processing Laboratory
Baltimore, Maryland 21250
and
National Chung Hsing University
Department of Electrical Engineering
Taichung, Taiwan, Republic of China

Jing Wang, MEMBER SPIE
University of Maryland Baltimore County
Department of Computer Science and Electrical Engineering
Remote Sensing Signal and Image Processing Laboratory
Baltimore, Maryland 21250

Chein-Chi Chang
University of Maryland Baltimore Country
Department of Civil and Environmental Engineering
Baltimore, Maryland 21250

Chinsu Lin
National Chiayi University
Department of Forestry
Environment Monitoring and Planning Laboratory
300 University Road
Chiayi 600 Taiwan, Republic of China

Abstract. Spectral signature coding is an effective means of characterizing spectral features. This paper develops a rather different encoding concept, called progressive signature coding (PSC), which encodes a signature in a hierarchical manner. More specifically, it progressively encodes a spectral signature in multiple stages; each of these stages captures disjoint spectral information contained in the spectral signature. As a result of this progressive coding, a spectral profile of progressive changes in a spectral signature can be generated for spectral characterization. The proposed idea is very simple and evolved from the pulse code modulation (PCM) commonly used in communications and signal processing. It expands PCM to multistage PCM (MPCM) in the sense that a signature can be decomposed and quantized by PCM progressively in multiple stages for spectral characterization. In doing so, the MPCM generates a priority code for a spectral signature so that its spectral information captured in different stages can be prioritized in accordance with significance of changes in spectral variation. Such MPCM-based progressive spectral signature coding (MPCM-PSSC) can be useful in applications such as hyperspectral data exploitation, environmental monitoring, and chemical/biological agent detection. Experiments are provided to demonstrate the utility of the MPCM-PSSC in signature discrimination and identification. [DOI: 10.1117/1.2353113]

Subject terms: multistage pulse code modulation (MPCM); MPCM-based progressive spectral signature coding (MPCM-PSSC); progressive spectral signature coding (PSSC); spectral signature coding (SSC); spectral discrimination; spectral identification.

Paper 050881R received Nov. 6, 2005; revised manuscript received Feb. 8, 2006; accepted for publication Feb. 17, 2006; published online Sep. 27, 2006.

1 Introduction

Spectral signature coding (SSC) is a scheme or a rule or a mapping that transforms spectral values into a new set of symbols in a specific manner such that a signature can be represented by the new symbols more effectively or efficiently. In hyperspectral imagery, each pixel is acquired by hundreds of contiguous spectral channels to form a column vector that can be used to diagnose subtle material substances based on their spectral characteristics. Therefore, taking advantage of such intrapixel spectral information (e.g., spectral information provided by spectral channels within a hyperspectral image pixel vector) is one of great benefits resulting from hyperspectral data. However, this comes at the price that many unknown spectral signatures may be also extracted to further complicate spectral analysis. So, one of major challenges in hyperspectral data exploitation is how to best utilize the spectral information provided by hyperspectral imagery to accomplish tasks such as detection, discrimination, classification, and identification while discarding undesired information caused by unwanted interference such as noise.

This paper investigates a new approach to SSC, called progressive spectral signature coding (PSSC), where the SSC is carried out in a progressive fashion rather than as sequential coding. It is a technique that can decompose a signature in multiple stages, each of which captures spectral changes in a progressive manner.[1–3] As a consequence, it provides a profile of progressive changes in spectral variation that describes the spectral behavior of a pixel vector in various stages. Accordingly, we can consider PSSC as *soft* coding in a progressive procedure, as opposed to SSC, which can be viewed as *hard* coding performed by classical coding techniques with binary decisions.

This paper develops a technique, called multistage pulse code modulation (MPCM) for PSSC (MPCM-PSSC), which was previously developed for progressive image compression.[4] The success of MPCM has been also dem-

0091-3286/2006/$22.00 © 2006 SPIE

onstrated in image progressive reconstruction,[5,6] progressive edge detection[7,8] and progressive text detection.[9] It is in fact a one-dimensional (1-D) transform coding technique, which encodes a 1-D signal progressively according to a priority assigned to each signal point. The signal priorities are determined by changes between two successive signal points. Interestingly, a hyperspectral image pixel can be also considered as a 1-D signal function.[10,11] As a consequence, each signal point corresponds to the spectral value of a particular wavelength in spectral dimension. With this interpretation, the MPCM can be implemented to capture progressive changes of spectral variation occurring at spectral wavelengths that are used to acquire the pixel.

One major advantage of using the PSSC is characterization of a spectral signature in progressive changes across its spectral channels. This unique feature cannot be accomplished by any hard-coding-based spectral coding methods. Another advantage is that the spectral profile of progressive changes produced for a signature can be used for various applications such as discrimination, classification, or identification. It is often the case that two signatures are very similar in the spectral signature vector direction measured by a spectral angle mapper (SAM),[11,12] but in fact have very different spectral profiles of progressive changes in a range of spectral channels. The PSSC provides such a profile for signature characterization. A third advantage is its use for change detection, which is a major task in land-cover remote sensing image classification and has been generally performed by temporal processing. The PSSC offers a different perspective on change detection in terms of spectral variation. A fourth advantage is that it can be viewed as a progressive implementation of a sequence of binary coding with a set of decreasing thresholds.

The proposed MPCM-PSSC provides a new look at how a SSC can be accomplished progressively for signature characterization. The idea is derived from the success of the MPCM in text detection for video images,[9] where the edges of text were detected more effectively in a progressive manner. Such progressive edge detection seems to be very useful in hyperspectral signature characterization. It generates a priority code that keeps track of progressive changes in spectral variation. The larger the change in a spectral wavelength is, the higher the priority of this particular wavelength is. Such an MPCM-PSSC-generated priority code provides fingerprints of a spectral signature via priority *code words* assigned to each of spectral wavelengths. Here, the term "code" refers to a codebook, which is made up of code words that are used for encoding. Another important advantage resulting from the MPCM-PSSC-generated priority code is progressive decomposition of a spectral signature in accordance with the priority code words assigned to each spectral wavelength. The resulting progressive decomposition delineates a profile of progressive changes in spectral variation that can be used for discrimination and identification of a spectral signature, a feature that cannot be achieved by any spectral similarity measure. Furthermore, the MPCM-PSSC-generated priority code can progressively reconstruct a spectral signature simply by the priority code words assigned to spectral wavelengths. This progressive signature reconstruction enables one to see how spectral changes are updated in order to recover the original signature from the MPCM-generated priority code. Most importantly, the MPCM-PSSC priority code can describe progressive transitions of spectral values from one spectral band to another via a simple coding scheme with a detailed profile of a spectral signature in terms of progressive changes in spectral variation across spectral wavelengths. Such capability makes the MPCM-PSSC unique. It distinguishes the MPCM-PSSC from a spectral similarity measure, which can only measure the closeness or similarity between two spectral signatures, not progressive spectral signature similarity across spectral wavelengths.

In order to facilitate analysis, a distinction between discrimination and identification, suggested in Ref. 11, is also made clear in this paper. The former is performed among a set of signatures, so that one signature is discerned from another, whereas the latter is performed by verifying a signature via a database (spectral library). Consequently, algorithms designed for discrimination and identification are slightly different. In particular, a threshold is generally required for signature discrimination to discriminate one signature from another. On the other hand, signature identification via a database can be performed directly by finding the signature in the database that best matches the signature to be identified. In our proposed MPCM-PSSC, the signature discrimination and signature matching are measured by priority code words using the Hamming distance. Finally, computer simulations and real data experiments are conducted to demonstrate the utility of the MPCM-PSSC in applications of signature discrimination and identification.

The remainder of this paper is organized as follows. Section 2 describes the MPCM encoding scheme in detail. Section 3 presents an MPCM-based progressive spectral signature coding (MPCM-PSSC) and develops algorithms for discrimination and identification. Section 4 conducts extensive experiments to substantiate the proposed MPCM-PSSC. Section 5 summarizes the results and conclusions with some remarks.

2 Multistage Pulse Code Modulation

In this section, we present a new concept, called *multistage pulse coding modulation* (MPCM), that can be used for encoding spectral signatures in a progressive manner. MPCM was originally developed for image progressive transmission and reconstruction.[4–6] It can be viewed as a progressive version of a commonly used coding scheme in communications, pulse code modulation (PCM).[13] It expands the hard-decision PCM-based quantizer to a soft-decision quantizer in such a fashion that it allows PCM to have a nondecision region, which passes on its decisions progressively to the next stage. As a result, a decision can be refined stage by stage so as to improve the quantization results.

The idea of multistage coding is not new and can be found in Ref. 13, in which many references are available, such as to tree or residual coding,[2,3,13,14] and multiresolution decomposition.[15] Nevertheless, the MPCM is new and quite different from the reported references in that it makes use of priority code words derived from multiple stages for progressive coding. The detailed idea of the MPCM can be described as follows.

A PCM-based coder is a quantizer, denoted by $Q(x)$, which is specified by a set of quantization levels $\{\Delta_k\}_{k=1}^{M}$

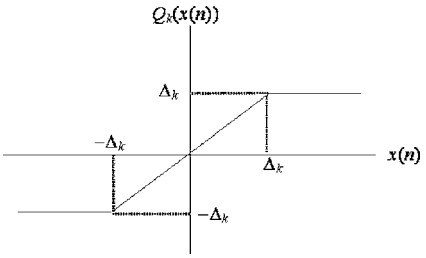

Fig. 1 A soft quantizer $Q_k(x(n))$ described by Eq. (2).

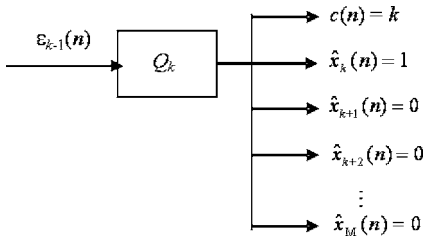

Fig. 2 Case 1 for MPCM encoding algorithm.

and a corresponding set of quantization thresholds $\{\tau_k\}_{k=1}^M$. It quantizes a signal function $x(n)$ according to

$$Q(x(n)) = \Delta_k \qquad \text{if } x(n) \in [\tau_{k-1}, \tau_k), \tag{1}$$

where Δ_0 and Δ_M are initial conditions determined by the domain of the signal function $x(n)$. It is a hard-decision-based quantizer, referred to as a hard quantization, because $Q(x(n))$ must make a decision on the input $x(n)$ via Eq. (1) by assigning the quantization level Δ_k to $x(n)$. The proposed MPCM expands $Q(x)$ in the sense that $x(n)$ in Eq. (1) is encoded by a sequence of M soft-decision-based quantizers $\{Q_k(x(n))\}_{k=1}^M$ in multiple stages, referred to as soft quantizers, in a progressive manner, as opposed to the hard decision made by one single value Δ_k in Eq. (1). Unlike the hard-decision-based quantizer described in Eq. (1), which makes its binary decision on $x(n)$ by means of a single threshold interval $[\tau_{k-1}, \tau_k)$ for each quantization level Δ_k, $Q_k(x(n))$ makes its decision based on three threshold intervals, $(-\infty, -\Delta_k]$, $(-\Delta_k, \Delta_k)$, and $[\Delta_k, \infty)$, determined by its quantization level Δ_k, where the interval $(-\Delta_k, \Delta_k)$ is designated as a no-decision threshold interval. More specifically, a soft quantizer $Q_k(x(n))$ derived from $Q(x(n))$ via the k'th quantization level Δ_k is defined by

$$Q_k(x(n)) = \begin{cases} -\Delta_k & \text{if } x(n) \in (-\infty, -\Delta_k], \\ x(n) & \text{if } x(n) \in (-\Delta_k, \Delta_k), \\ \Delta_k & \text{if } x(n) \in [\Delta_k, \infty), \end{cases} \tag{2}$$

where the soft quantizer $Q_k(x(n))$ passes its input $x(n)$ without making any decision when the input $x(n)$ falls in the region $x(n) \in (-\Delta_k, \Delta_k)$ as described in Fig. 1. The consequence of soft decisions comes from the inclusion of the no-decision interval $(-\Delta_k, \Delta_k)$ in the quantizer $Q_k(x(n))$.

The MPCM takes advantage of the soft quantizer $Q_k(x(n))$ specified by Eq. (2) to perform quantization progressively in multiple stages specified by $\{\Delta_k\}_{k=1}^M$, referred to as *stage levels* in the MPCM. Assume that $\{\Delta_k\}_{k=1}^M$ are strictly decreasing quantization levels, i.e., $\Delta_1 > \Delta_2 > \cdots > \Delta_M > 0$. Therefore, the no-decision-made outputs passed by the k'th soft quantizer $Q_k(x(n))$ at stage k are further processed by the follow-up $(k+1)$st soft quantizer $Q_{k+1}(x(n))$ in the next stage, which uses a smaller quantization level, $\Delta_{k+1} < \Delta_k$ to refine its decision. In other words, instead of encoding $x(n)$ directly into Δ_k by Eq. (1), $x(n)$ is actually encoded by M soft quantizers $\{Q_k(x(n))\}_{k=1}^M$ one at a time, progressively using M refined quantization levels. As a result of using a sequence of progressive soft quantizers $\{Q_k(x(n))\}_{k=1}^M$, $x(n)$ can be decomposed into a set of binary-valued stage components, denoted by $\{\hat{x}_k(n)\}_{k=1}^M$ where $\hat{x}_k(n) \in \{0,1\}$ for $1 \leq k \leq M$, so that the $x(n)$ can be approximated by the estimate $\hat{x}(n)$ of $x(n)$ given by

$$\hat{x}(n) = \hat{x}_1\Delta_1 + \hat{x}_2\Delta_2 + \cdots + \hat{x}_M\Delta_M = \sum_{k=1}^{M} \hat{x}_k(n)\Delta_k. \tag{3}$$

The key task is to find the desired set of M soft binary quantizers, $\{Q_k(x(n))\}_{k=1}^M$ for a given set of quantization levels $\{\Delta_k\}_{k=1}^M$ to produce an optimal M-block-length binary code for Eq. (3) in approximation. In doing so, the soft quantizer using the quantization level Δ_k defined by Eq. (2) can be used for the k'th progressive soft quantizer in the MPCM defined by

$$Q_k(\varepsilon_{k-1}(n)) = \begin{cases} -\Delta_k & \text{if } \varepsilon_{k-1}(n) \in (-\infty, -\Delta_k], \\ \varepsilon_{k-1}(n) & \text{if } \varepsilon_{k-1}(n) \in (-\Delta_k, \Delta_k), \\ \Delta_k & \text{if } \varepsilon_{k-1}(n) \in [\Delta_k, \infty), \end{cases} \tag{4}$$

which takes as its input the approximation error $\varepsilon_{k-1}(n) = x(n) - \sum_{j=1}^{k-1} \hat{x}_j(n)\Delta_j$ obtained at the $(k-1)$st stage. It should be noted that $\varepsilon_{k-1}(n)$ used in Eq. (4) is the approximation error obtained by successive approximations using the binary code word $(\hat{x}_1(n)\hat{x}_2(n)\cdots\hat{x}_M(n))$ up to the $(k-1)$st stage. The soft decision comes from the case that if $\varepsilon_{k-1}(n) \in (-\Delta_k, \Delta_k)$, then $Q_k(\varepsilon_{k-1}(n)) = \varepsilon_{k-1}(n)$.

A detailed implementation of the MPCM is described as follows. A generalized version of MPCM can be found in Refs. 4–6.

MPCM encoding algorithm for the n'th signal point $x(n)$.

1. *Initial condition*: Let $\{\Delta_k\}_{k=1}^M$ be a set of M stage levels that are used for MPCM, and the initial approximation error be $\varepsilon_0(n) = x(n) - \hat{x}(n-1)$, where $\hat{x}(n-1)$ is obtained by Eq. (3). Set $\hat{x}(0) = 0$ and $k = 1$.
2. At the k'th stage, three cases are considered for the k'th two-valued soft quantizer Q_k defined by Eq. (4):

   Case 1. If $\varepsilon_{k-1}(n) \geq \Delta_k$, then $Q_k(\varepsilon_{k-1}(n)) = \Delta_k$, $\hat{x}_k(n) = 1$; set $\hat{x}_j(n) = 0$ for $k < j \leq M$. In this case, the priority code word $c(n)$ assigned to $x(n)$ is $c(n) = k$. Its diagram is depicted in Fig. 2.

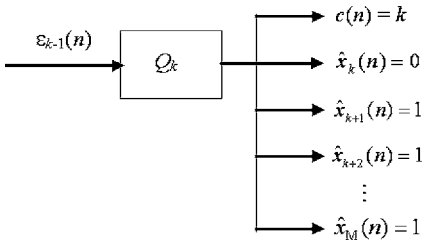

Fig. 3 Case 2 for MPCM encoding algorithm.

Let $\varepsilon_M(n)=\varepsilon_{k-1}(n)-\Sigma_{j=k}^{M}\hat{x}_j(n)\Delta_j=\varepsilon_{k-1}(n)-\Delta_k$. Go to step 4.

Case 2. If $\varepsilon_{k-1}(n)\leq-\Delta_k$, then $Q_k(\varepsilon_{k-1}(n))=-\Delta_k$, $\hat{x}_k(n)=0$; set $\hat{x}_j(n)=1$ for $k<j\leq M$. In this case, the priority code word $c(n)$ assigned to $x(n)$ is $c(n)=k$. Its diagram is depicted in Fig. 3. Let $\varepsilon_M(n)=\varepsilon_{k-1}(n)-\Sigma_{j=k}^{M}\hat{x}_j(n)\Delta_j=\varepsilon_{k-1}(n)-\Sigma_{j=k+1}^{M}\Delta_k$. Go to step 4.

Case 3. If $-\Delta_k<\varepsilon_{k-1}(n)<\Delta_k$, then $Q_k(\varepsilon_{k-1}(n))=\varepsilon_{k-1}(n)$ and $\hat{x}_k(n)=\hat{x}_k(n-1)$. Its diagram is depicted in Fig. 4. Go to step 3.

3. If $k<M$, let $k=k+1$ and go to step 2. Otherwise, continue.
4. Go to the next sample, $(n+1)$st signal point, $x(n+1)$.

In this MPCM encoding algorithm, the priority code word is only assigned when a hard decision is made in a certain stage. When it occurs at stage k, the encoding for $x(n)$ is terminated and the priority code word for $x(n)$ is encoded as $c(n)=k$. In this case, the priority assigned to $x(n)$ is k, which indicates that there is a significant change in $x(n)$ at stage k. As a result, the higher the priority is, the greater the change is, and the smaller the index number of the stage is. That is, $c(n)=1$ has the highest priority, since there is a drastic change in stage 1 specified by the largest quantization level Δ_1. To the contrary, $c(n)=M$ indicates that there only has been a small change in stage M, because the quantization level Δ_M is the smallest one. Interestingly, an immediate advantage resulting from the MPCM encoding algorithm is that it allows one to decompose a signal sample $x(n)$ in multiple stages, viz., M stages, and its priority code word indicates in which stage the priority occurs—where the signal sample makes a significant change.

Correspondingly, we also describe the MPCM decoding algorithm as follows. It decodes the n'th signal sample $x(n)$ according to the encoded priority code word $c(n)$ along with the previous decoded $\hat{x}(n-1)$, which is an approximation of $x(n-1)$ via Eq. (3). In contrast to the MPCM encoding algorithm, which decomposes the n'th signal sample

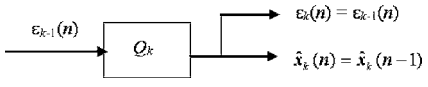

Fig. 4 Case 3 for MPCM encoding algorithm.

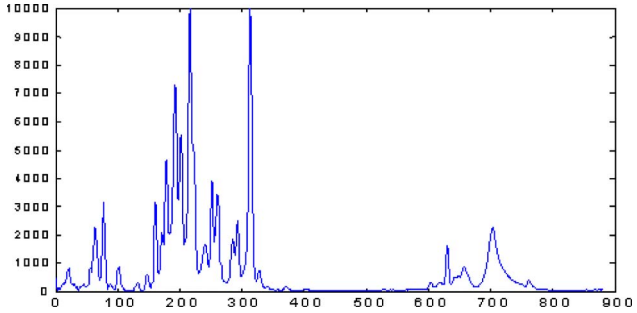

Fig. 5 Spectral signature of methyl salicylate, **r**.

stage by stage in M stages, the MPCM decoding algorithm reconstructs the n'th signal samples stage by stage according to its priority code word $c(n)$.

MPCM decoding algorithm for $x(n)$.

1. *Initial condition*: Let $\{\Delta_k\}_{k=1}^{M}$ be a set of M stage levels that are used for MPCM. Set the initial condition as $\hat{x}(0)=0$, and let $\hat{x}(n-1)$ be the reconstruction of $x(n)$, which is unknown and can be expressed by $\{\hat{x}_k(n-1)\}_{k=1}^{M}$ as

$$\hat{x}(n-1)=\hat{x}_1(n-1)\Delta_1+\hat{x}_2(n-1)\Delta_2+\cdots+\hat{x}_M(n-1)\Delta_M. \quad (5)$$

2. Input the encoded priority code word $c(n)=k$ for $x(n)$, in which case the priority of $x(n)$ occurs in stage k. Two cases are considered.

Case 1. If $\hat{x}_k(n-1)=1$, then $\hat{x}_j(n)=\hat{x}_j(n-1)$ for $1\leq j<k$, $\hat{x}_k(n)=0$, and $\hat{x}_j(n)=1$ for $k<j<M$. In this case, $\hat{x}(n)=\Sigma_{j=1}^{k-1}\hat{x}_j(n-1)\Delta_j+\Sigma_{j=k+1}^{M}\Delta_j$.

Case 2. If $\hat{x}_k(n-1)=0$, then $\hat{x}_j(n)=\hat{x}_j(n-1)$ for $1\leq j<k$, $\hat{x}_k(n)=1$, and $\hat{x}_j(n)=0$ for $k<j<M$. In this case, $\hat{x}(n)=\Sigma_{j=1}^{k-1}\hat{x}_j(n-1)\Delta_j+\Delta_k$.

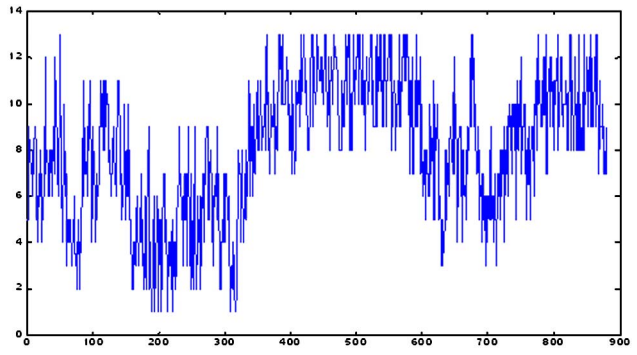

Fig. 6 Graphical plot of priority code words for the signature of methyl salicylate in Fig. 5. x-coordinates: band numbers; y-coordinates: priority code words.

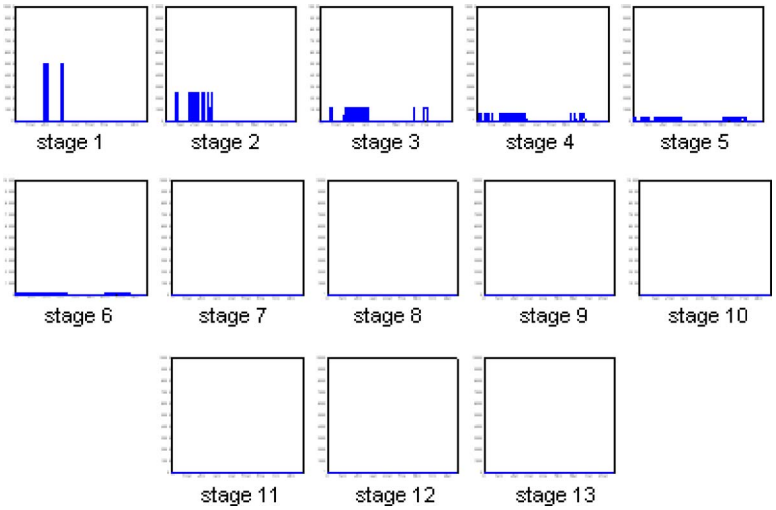

Fig. 7 MPCM-encoded progressive spectral signatures of methyl salicylate. x-coordinates: band numbers; y-coordinates: priority code words.

In order to apply the MPCM to spectral signature coding, we consider the spectrum of a signature vector $\mathbf{r}=(r_1,r_2,\ldots,r_L)^T$ as a 1-D signature vector with r_l the spectral value of the l'th band. Let $\Delta(\mathbf{r})=\max_l\{r_l\}-\min_l\{r_l\}$. The number of stages, M, is then given by

$$M=[\log_2 \Delta(\mathbf{r})]+1 \tag{6}$$

with $[x]$ defined as the largest integer less than or equal to x. So, the stage levels $\{\Delta_k\}_{k=1}^{M}$ used in the MPCM are defined by

$$\Delta_k(\mathbf{r})=2^{-k}\Delta(\mathbf{r}) \qquad \text{for } k=1,2,\ldots,M. \tag{7}$$

In order to demonstrate the utility of the MPCM in spectral signature coding, two examples are provided for illustration.

The first example shows a progressive MPCM-encoded signal of a 1-D chemical spectral data vector $\mathbf{r}$, methyl salicylate, obtained from the Web book of the National Institute of Standards and Technology (NIST).[16] It is shown in Fig. 5 and has 880 bands of spectral coverage from 450 to 3966 cm^{-1}.

In order for the MPCM to operate on this signal, the number of stages required for the MPCM encoding was calculated by Eq. (6) to be $M=13$ stages. Since there are 13 stages, the stage levels obtained by Eq. (7) are $\Delta_k=\Delta(\mathbf{r})/2^k$ for $k=1,2,\ldots,13$. The initial condition is assumed to be $x(0)=0$. Figure 6 shows a graphical plot of the priority code words $c(n)$ for each of signal points $x(n)$ in Fig. 5 produced by the MPCM encoding algorithm with the x axis and y axis specified by signal points and their corresponding priority code words ranging from 1 to 13. Using the MPCM encoded priority code words provided by Fig. 6, a 13-stage progressive decomposition into signal components of the original signal in Fig. 5 can be obtained as in Fig. 7. As we can see from Fig. 7, the MPCM encoding algorithm started with the highest stage level, $\Delta_1=(2^{13}/2)\times\{\Delta(\mathbf{r})/2^{13}\}=4096\times\{\Delta(\mathbf{r})/2^{13}\}$, in stage 1, and then reduced stage levels by factors of 2 to refine signal samples until it reached the last stage, which is stage 13 specified by stage level $\Delta_{13}=\Delta(\mathbf{r})/2^{13}$.

In order to decode the signal of methyl salicylate, the MPCM-encoded priority code words in Fig. 6 were used as inputs, and Fig. 8 shows the 13 decoded signal components of methyl salicylate for stage-by-stage signature reconstruction along with the approximation error $\varepsilon_{13}(n)$.

Since it may not be trivial to fully understand how the MPCM works, a second example is provided by Table 1 for illustration. It takes the first 20 signal points in Fig. 5 and walks through detailed stage-by-stage implementations of the MPCM encoding and decoding algorithms.

In Table 1, the first set of columns lists the inputs specified by the first 20 signal points $\{x(n)\}_{n=1}^{20}$ with the initial

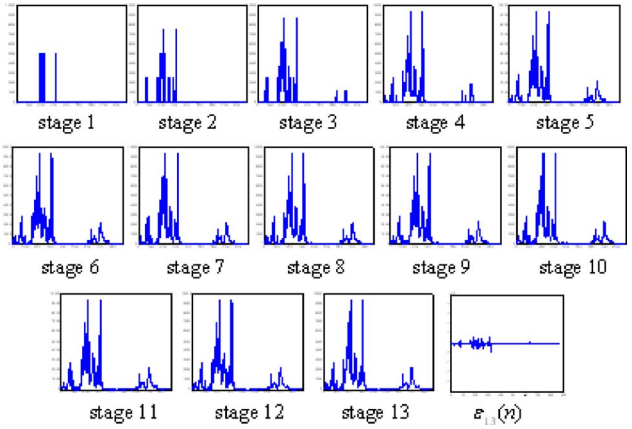

Fig. 8 Stage-by-stage decoded spectral signatures of methyl salicylate from the priority code words in Fig. 6, along with the approximation error $\varepsilon_{13}(n)$. x-coordinates: band numbers; y-coordinates: priority code words.

Table 1 The first 20 MPCM-encoded signal samples in Fig. 5, using 13 stages for signal decomposition.

Input		Prediction		Signal components													Output
n	$x(n)$	$\hat{x}(n)$	$\varepsilon(n)$	$\hat{x}_1$	$\hat{x}_2$	$\hat{x}_3$	$\hat{x}_4$	$\hat{x}_5$	$\hat{x}_6$	$\hat{x}_7$	$\hat{x}_8$	$\hat{x}_9$	$\hat{x}_{10}$	$\hat{x}_{11}$	$\hat{x}_{12}$	$\hat{x}_{13}$	$c(n)$
0	0	0	0	0	0	0	0	0	0	0	0	0	0	0	0	0	0
1	367	256	111	0	0	0	0	1	0	0	0	0	0	0	0	0	5
2	144	255	−111	0	0	0	0	0	1	1	1	1	1	1	1	1	5
3	33	127	−94	0	0	0	0	0	0	1	1	1	1	1	1	1	6
4	108	111	−3	0	0	0	0	0	0	1	1	0	1	1	1	1	9
5	70	95	−25	0	0	0	0	0	0	1	0	1	1	1	1	1	8
6	106	96	10	0	0	0	0	0	0	1	1	0	0	0	0	0	8
7	59	63	−4	0	0	0	0	0	0	0	1	1	1	1	1	1	7
8	119	64	55	0	0	0	0	0	0	1	0	0	0	0	0	0	7
9	157	128	29	0	0	0	0	0	1	0	0	0	0	0	0	0	6
10	162	160	2	0	0	0	0	0	1	0	1	0	0	0	0	0	8
11	198	192	6	0	0	0	0	0	1	1	0	0	0	0	0	0	7
12	233	224	9	0	0	0	0	0	1	1	1	0	0	0	0	0	8
13	240	240	0	0	0	0	0	0	1	1	1	1	0	0	0	0	9
14	223	223	0	0	0	0	0	0	1	1	0	1	1	1	1	1	8
15	245	224	21	0	0	0	0	0	1	1	1	0	0	0	0	0	8
16	290	256	34	0	0	0	0	1	0	0	0	0	0	0	0	0	5
17	388	384	4	0	0	0	0	1	1	0	0	0	0	0	0	0	6
18	516	512	4	0	0	0	1	0	0	0	0	0	0	0	0	0	4
19	591	576	15	0	0	0	1	0	0	1	0	0	0	0	0	0	7
20	665	640	25	0	0	0	1	0	1	0	0	0	0	0	0	0	6

condition specified by $x(0)=0$. The second set lists the values of predicted $\hat{x}(n)$ and predicted error $\varepsilon(n)$. The third set lists all predicted values of signal components in 13 stages with stage levels specified by the largest stage level, $\Delta_1=2^{12}=4096$, down to the smallest stage level, $\Delta_{13}=2^0=1$. Finally, the last column lists the priority code words $\{c(n)\}_{n=1}^{20}$ for the first 20 signal points, $\{x(n)\}_{n=1}^{20}$.

Table 2 provides a stage-by-stage decoding process for signal reconstruction of the 20 MPCM signal samples encoded in Table 1, where the first set of columns takes the priority code words from the output in Table 1 as the input to the MPCM decoder to decode the signal components in all 13 stages in the second set of columns. Finally, the last column of Table 2 lists the predicted values of all the first 20 signal points of $\{x(n)\}_{n=1}^{20}$.

To conclude this section, two comments are noteworthy. In order to implement the MPCM-PSSC, a set of parameters, such as the stage levels $\{\Delta_k\}_{k=1}^{M}$, is required *a priori*. A general approach to such selection is given by Eq. (7), which is empirically reasonable in our experiments. Another comment is that the computational complexity of the MPCM-PSSC is simple. As a matter of fact, it can be implemented as a real-time process for progressive transmission.

3 MPCM-Based Progresssive Spectral Signature Coding

As recalled in the MPCM encoding algorithm, a signature vector $\mathbf{r}=(r_1,r_2,\ldots,r_L)^T$ will be considered as a 1-D spectral signature where r_l is represented by one of the priority code words $\{c_k(\mathbf{r})\}_{k=1}^{M}$ with $c_k(\mathbf{r})$ taking values in $\{1,2,\ldots,M\}$. For example, $c_l(\mathbf{r})$ indicates the priority of r_l

Table 2 The first 20 MPCM decoded signal points for the signal reconstruction in Fig. 5 with 13 stages.

Input		Signal components													
n	$c(n)$	$\hat{x}_1$	$\hat{x}_2$	$\hat{x}_3$	$\hat{x}_4$	$\hat{x}_5$	$\hat{x}_6$	$\hat{x}_7$	$\hat{x}_8$	$\hat{x}_9$	$\hat{x}_{10}$	$\hat{x}_{11}$	$\hat{x}_{12}$	$\hat{x}_{13}$	Output $\hat{x}(n)$
0	0	0	0	0	0	0	0	0	0	0	0	0	0	0	0
1	5	0	0	0	0	1	0	0	0	0	0	0	0	0	256
2	5	0	0	0	0	0	1	1	1	1	1	1	1	1	255
3	6	0	0	0	0	0	0	1	1	1	1	1	1	1	127
4	9	0	0	0	0	0	0	1	1	0	1	1	1	1	111
5	8	0	0	0	0	0	0	1	0	1	1	1	1	1	95
6	8	0	0	0	0	0	0	1	1	0	0	0	0	0	96
7	7	0	0	0	0	0	0	0	1	1	1	1	1	1	63
8	7	0	0	0	0	0	0	1	0	0	0	0	0	0	64
9	6	0	0	0	0	0	1	0	0	0	0	0	0	0	128
10	8	0	0	0	0	0	1	0	1	0	0	0	0	0	160
11	7	0	0	0	0	0	1	1	0	0	0	0	0	0	192
12	8	0	0	0	0	0	1	1	1	0	0	0	0	0	224
13	9	0	0	0	0	0	1	1	1	1	0	0	0	0	240
14	8	0	0	0	0	0	1	1	0	1	1	1	1	1	223
15	8	0	0	0	0	0	1	1	1	0	0	0	0	0	224
16	5	0	0	0	0	1	0	0	0	0	0	0	0	0	256
17	6	0	0	0	0	1	1	0	0	0	0	0	0	0	384
18	4	0	0	0	1	0	0	0	0	0	0	0	0	0	512
19	7	0	0	0	1	0	0	1	0	0	0	0	0	0	576
20	6	0	0	0	1	0	1	0	0	0	0	0	0	0	640

in the MPCM encoding and decoding. The smaller the number $c_l(\mathbf{r})$ is, the higher priority the r_l is for spectral encoding and decoding.

Next, we can further construct an M-dimensional priority unit vector associated with the priority code word $c_l(\mathbf{r})$ for MPCM-PSC as follows:

$$\mathbf{c}_l(\mathbf{r}) = (c_{l1}(\mathbf{r}), c_{l2}(\mathbf{r}), \ldots, c_{lM}(\mathbf{r}))^T \tag{8}$$

with $c_{lk}(\mathbf{r}) \in \{0,1\}$ and $\sum_{k=1}^{M} c_{lk}(\mathbf{r}) = 1$. The condition that $\sum_{k=1}^{M} c_{lk}(\mathbf{r}) = 1$ in Eq. (8) implies that $\mathbf{c}_l(\mathbf{r})$ is the only one component with 1 component and all zeros for its remaining components. It should be noted that the priority code word $c_l(\mathbf{r})$ takes its value in $\{1,2,\ldots,M\}$. Instead of using the priority code word $c_l(\mathbf{r})$ itself, we use its corresponding M-dimensional priority unit vector $\mathbf{c}_l(\mathbf{r})$ defined by Eq. (8), where the boldface version $\mathbf{c}_l(\mathbf{r})$ of $c_l(\mathbf{r})$ indicates that it is the priority unit vector of the original scalar priority code word $\mathbf{c}_l(\mathbf{r})$. As an example, for $M=8$, $c_l(\mathbf{r})$ can take any of eight values, 1, 2, 3, 4, 5, 6, 7, 8. In this case, the following eight-dimensional priority unit vectors derived from Eq. (8) can be used for spectral signature coding:

$$c_l(\mathbf{r}) = 1 \Leftrightarrow \mathbf{c}_l(\mathbf{r}) = (1,0,0,0,0,0,0,0),$$

$$c_l(\mathbf{r}) = 2 \Leftrightarrow \mathbf{c}_l(\mathbf{r}) = (0,1,0,0,0,0,0,0),$$

$$c_l(\mathbf{r}) = 3 \Leftrightarrow \mathbf{c}_l(\mathbf{r}) = (0,0,1,0,0,0,0,0),$$

$$c_l(\mathbf{r}) = 4 \Leftrightarrow \mathbf{c}_l(\mathbf{r}) = (0,0,0,1,0,0,0,0),$$

$$c_l(\mathbf{r}) = 5 \Leftrightarrow \mathbf{c}_l(\mathbf{r}) = (0,0,0,0,1,0,0,0),$$

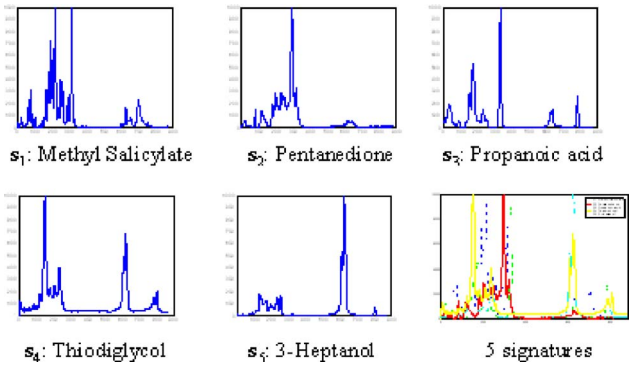

Fig. 9 Five spectral signatures of chemical data from NIST. x-coordinates: band numbers; y-coordinates: priority code words.

$$c_l(\mathbf{r}) = 6 \Leftrightarrow \mathbf{c}_l(\mathbf{r}) = (0,0,0,0,0,1,0,0),$$

$$c_l(\mathbf{r}) = 7 \Leftrightarrow \mathbf{c}_l(\mathbf{r}) = (0,0,0,0,0,0,1,0),$$

$$c_l(\mathbf{r}) = 8 \Leftrightarrow \mathbf{c}_l(\mathbf{r}) = (0,0,0,0,0,0,0,1). \tag{9}$$

More specifically, if the priority code word $c_l(\mathbf{r})$ resulting from r_l is the priority k, its M-dimensional priority unit vector $\mathbf{c}_l(\mathbf{r})$ is then specified by

$$\mathbf{c}_l(\mathbf{r}) = (\underbrace{0}_{1},\underbrace{0}_{2},\ldots,\underbrace{0}_{k-1},\underbrace{1}_{k},\underbrace{0}_{k+1},\ldots,\underbrace{0}_{M-1},\underbrace{0}_{M})^T, \tag{10}$$

where only 1 occurs in the k'th component and represents its priority specified by the k'th stage. The advantage of using the M-dimensional priority unit vector is that the position of the 1 in Eq. (10) indicates the significance of its priority in the same manner that the bit position indicates the precision of the bit in a binary representation. Most importantly, we can use Eq. (10) and the Hamming distance to define a distance measure between two signature vectors $\mathbf{r}=(r_1,r_2,\ldots,r_L)^T$ and $\mathbf{s}=(s_1,s_2,\ldots,s_L)^T$ at the k'th stage via their corresponding M-dimensional priority unit vectors by

$$D_k(\mathbf{r},\mathbf{s}) = \sum_{l=1}^{L} c_{lk}(\mathbf{r}) \oplus c_{lk}(\mathbf{s}). \tag{11}$$

where there is an $\oplus$ exclusive OR.

3.1 *Spectral Discrimination*

By virtue of Eq. (11), the similarity between two signature vectors $\mathbf{r}$ and $\mathbf{s}$ can be measured progressively. In other words, two signature vectors $\mathbf{r}$ and $\mathbf{s}$ are first measured by Eq. (11) in stage 1 via a prescribed stage threshold, say Δ_1. If the distance $D_1(\mathbf{r},\mathbf{s})$ is greater than Δ_1, then $\mathbf{r}$ and $\mathbf{s}$ will be declared to be distinct. Otherwise, the comparison between $\mathbf{r}$ and $\mathbf{s}$ is continued to proceed at stage 2. If the distance $D_2(\mathbf{r},\mathbf{s})$ is greater than a prescribed stage threshold Δ_2, then $\mathbf{r}$ and $\mathbf{s}$ will be considered to be distinct signatures. Otherwise, a further comparison between $\mathbf{r}$ and $\mathbf{s}$ is continued on at stage 3, etc. The implementation of the MPCM-based progressive spectral coding for target discrimination can be summarized as follows.

MPCM-PSSC spectral discrimination algorithm.

1. Let $\mathbf{r}$ and $\mathbf{s}$ be two spectral signature vectors to be discriminated.
2. Specify the number of stages, M, needing to be processed. If two signatures produce different stage numbers M_1 and M_2, then M is chosen as the minimum of M_1 and M_2.
3. Determine the stage thresholds $\{\tau_k\}_{k=1}^{M}$ to be used for discrimination in each of the M stages.
4. Apply the MPCM to $\mathbf{r}$ and $\mathbf{s}$ to generate their priority code words as described in Eq. (8) and expressed by Eq. (10).
5. Use Eq. (11) to measure the similarity between $\mathbf{r}$ and $\mathbf{s}$ progressively. For each stage k, we calculate the distance $D_k(\mathbf{r},\mathbf{s})$ and compare it against the k'th stage threshold, Δ_k. If $D_k(\mathbf{r},\mathbf{s}) > \tau_k$, the two pixel vectors $\mathbf{r}$ and $\mathbf{s}$ are declared to be distinct, and the process is terminated. Otherwise, repeat the same procedure until it reaches the last stage M. In this case, we check if $D_M(\mathbf{r},\mathbf{s}) > \tau_M$.
6. If $D_M(\mathbf{r},\mathbf{s}) > \tau_M$, the two pixel vectors $\mathbf{r}$ and $\mathbf{s}$ are declared to be distinct, and the process is terminated.
7. If $D_M(\mathbf{r},\mathbf{s}) \leqslant \tau_M$, the process is also terminated and the output is "no discrimination," which declares $\mathbf{r}$ and $\mathbf{s}$ to be the same signature.

A key issue in implementing the MPCM-PSSC discrimination algorithm is the determination of an appropriate set of M stage thresholds for a signature. In doing so a simu-

Table 3 Thirteen stage thresholds for five signatures in Fig. 9 with SNR 30 : 1.

Signature	τ_1	τ_2	τ_3	τ_4	τ_5	τ_6	τ_7	τ_8	τ_9	τ_{10}	τ_{11}	τ_{12}	τ_{13}
$\mathbf{s}_1$	2	3	7	16	23	28	40	47	58	58	54	48	47
$\mathbf{s}_2$	1	9	6	19	29	40	61	61	83	96	94	83	81
$\mathbf{s}_3$	2	3	6	10	21	27	38	49	50	57	70	66	64
$\mathbf{s}_4$	1	2	9	26	27	52	92	110	150	150	140	80	130
$\mathbf{s}_5$	0	0	1	5	8	18	20	30	37	55	55	58	87

Table 4 Discrimination among five signatures in Fig. 9 using the stage thresholds in Table 3.

Signatures	1	2	3	4	5	6	7	8	9	10	11	12	13
$\mathbf{s}_1$-$\mathbf{s}_2$	10	32	49	80	94	120	170	190	190	200	160	110	120
$\mathbf{s}_1$-$\mathbf{s}_3$	12	32	53	72	100	120	150	180	180	180	190	120	140
$\mathbf{s}_1$-$\mathbf{s}_4$	12	30	57	98	100	150	200	160	180	170	150	87	150
$\mathbf{s}_1$-$\mathbf{s}_5$	10	28	48	69	88	120	140	160	180	180	170	130	260
$\mathbf{s}_2$-$\mathbf{s}_3$	6	22	36	54	88	110	140	160	180	200	180	140	170
$\mathbf{s}_2$-$\mathbf{s}_4$	6	20	42	78	82	140	180	160	190	190	160	110	170
$\mathbf{s}_2$-$\mathbf{s}_5$	4	18	27	45	66	100	140	130	180	210	160	130	280
$\mathbf{s}_3$-$\mathbf{s}_4$	8	16	44	78	88	130	160	170	160	180	170	130	170
$\mathbf{s}_3$-$\mathbf{s}_5$	6	14	35	39	80	98	96	140	160	170	180	170	270
$\mathbf{s}_4$-$\mathbf{s}_5$	6	14	39	67	76	120	150	130	170	180	160	110	280

lated white Gaussian noise is added to the signature to achieve a certain signal-to-noise ratio (SNR). This SNR is determined by how much sensitivity we would like to have for a signature responding to its spectral variations.

3.2 *Spectral Identification*

The target identification studied in this section is different from the spectral discrimination in Sec. 3.1. While the target discrimination only discriminates one signature from another without performing any additional task such as detection, classification, or identification, the target identification uses a given database (spectral library) Γ to identify an unknown target signature $\mathbf{t}$. Unlike spectral discrimination, the proposed spectral identification does not require stage thresholds.

MPCM-PSSC spectral identification algorithm 1.

1. Let Γ be a given database (spectral library) that is made up of p spectral signatures $\mathbf{s}_1, \mathbf{s}_2, \ldots, \mathbf{s}_p$ (i.e., $\Gamma = \{\mathbf{s}_h\}_{h=1}^{p}$), and $\mathbf{t}$ be the target spectral signature vector to be identified via the database Γ.
2. Specify, via Eq. (6), the number of stages, M, needed to be processed. For each signature $\mathbf{s}_h$, let M_h be the associated stage number. Then M is chosen as the minimum among $M_1, M_2, \ldots, M_p$.
3. Determine stage thresholds for all M stages, $\{\tau_k\}_{k=1}^{M}$ for $\mathbf{s}_1, \mathbf{s}_2, \ldots, \mathbf{s}_p$.
4. Apply the MPCM to the target signature $\mathbf{t}$ to generate its priority code. Set $k=1$.
5. At the k'th stage, calculate the distance $D_k(\mathbf{t}, \mathbf{s}_h)$ between $\mathbf{t}$ and $\mathbf{s}_h$ at stage k for $1 \leqslant h \leqslant p$, using Eq. (11). The best $\mathbf{t}$ is identified by $\mathbf{s}_{h^*}$ with $h^* = \min_{1 \leqslant h \leqslant p}\{D_k(\mathbf{t}, \mathbf{s}_h)\}$. If there is a tie, the process is continued with those signatures that yield $\min_{1 \leqslant h \leqslant p}\{D_k(\mathbf{t}, \mathbf{s}_h)\}$.
6. If $k < M$, let $k \leftarrow k+1$ and go to step 5. Otherwise, continue.
7. In this case, we reach the last stage M. The best $\mathbf{t}$ is identified by $\mathbf{s}_{h^*}$ with $h^* = \min_{1 \leqslant h \leqslant p}\{D_M(\mathbf{t}, \mathbf{s}_h)\}$. If there is a tie at this final stage, the algorithm either declares "no match" or identifies $\mathbf{t}$ as one of the tied signatures.

Steps 5 to 7 in this algorithm calculate the distance

Table 5 Spectral identification for a mixed signature, $\mathbf{s} = 0.6\mathbf{t} + 0.1\mathbf{s}_2 + 0.1\mathbf{s}_3 + 0.1\mathbf{s}_4 + 0.1\mathbf{s}_5$ with $\mathbf{t} = \mathbf{s}_1$.

Signature	1	2	3	4	5	6	7	8	9	10	11	12	13	SUM
$\mathbf{s}_1$	6	24	46	80	110	120	140	170	140	130	130	70	68	1234
$\mathbf{s}_2$	12	34	47	88	100	130	170	170	190	190	150	99	120	1500
$\mathbf{s}_3$	14	34	55	92	110	130	150	170	170	170	180	130	150	1555
$\mathbf{s}_4$	14	30	61	110	110	170	200	160	170	160	140	79	160	1564
$\mathbf{s}_5$	12	30	46	77	95	130	140	150	180	170	160	120	270	1580

Table 6 Spectral identification for a mixed signature, $\mathbf{s}=0.1\mathbf{s}_1+0.6\mathbf{t}+0.1\mathbf{s}_3+0.1\mathbf{s}_4+0.1\mathbf{s}_5$ with $\mathbf{t}=\mathbf{s}_2$.

Signature	1	2	3	4	5	6	7	8	9	10	11	12	13	SUM
$\mathbf{s}_1$	10	32	53	87	120	150	180	190	170	170	160	96	98	1516
$\mathbf{s}_2$	0	16	22	59	98	130	140	160	150	190	150	110	100	1325
$\mathbf{s}_3$	6	20	42	65	100	130	150	190	160	180	170	130	160	1503
$\mathbf{s}_4$	6	18	48	83	110	160	190	180	170	160	150	95	150	1520
$\mathbf{s}_5$	4	16	31	54	96	120	130	150	170	180	170	120	290	1531

$D_k(\mathbf{t},\mathbf{s}_h)$ between $\mathbf{t}$ and $\mathbf{s}_h$ for each $1\leqslant h\leqslant p$ stage by stage and makes a progressive decision to determine if there is a match between $\mathbf{t}$ and $\mathbf{s}_{h^*}$ for some h^*. There is no need of implementing stage thresholds as with spectral discrimination. As an alternative, we can also replace steps 5 to 7 to derive a second version of MPCM-PSSC target identification that postpones the decision until the last stage M by calculating the sum of stage distances between $\mathbf{t}$ and $\mathbf{s}_h$ in all M stages. In this case, the identification is to find the signature that yields the smallest sum.

MPCM-PSSC spectral identification algorithm 2. The same first four steps used in MPCM-PSSC target identification algorithm 1 are followed by 5′. Compute $\mathrm{SUM}_h=\Sigma_{k=1}^{M}D_k(\mathbf{t},\mathbf{s}_h)$, and identify $\mathbf{t}$ by $\mathbf{s}_{h^*}$ with $h^*=\arg\{\min_{1\leqslant h\leqslant p}\{\mathrm{SUM}_h\}\}$, the signature that yields the smallest SUM_h. If there is a tie at this final stage, the algorithm either declares "no match" or identifies $\mathbf{t}$ as one of the tied signatures.

It should be noted that step 5′ does not make its decision progressively. Instead, it makes its decision at the final stage, M, based on the sum of all stage distances. Nevertheless, it does take advantage of the progressive spectral signature changes occurred at each stage, each of which contributes its change to the sum.

4 Data Experiments on Chemical/Biological Laboratory

The ability of the MPCM-PSSC in progressive signature decomposition and progressive signature reconstruction was demonstrated in Figs. 7 and 8 and Tables 1 and 2. This and the following sections further demonstrate the versatility of the MPCM-PSSC in other applications: spectral discrimination and identification. Two sets of data were used for experiments: laboratory data and real hyperspectral images. The laboratory data used in this section are chemical/biological spectral data available online at NIST's Web site.[16] The data set has the five 880-band chemical/biological spectral signatures shown in Fig. 9, which are for methyl salicylate, pentanedione, propanoic acid, thiodiglycol, and 3-heptanol. The selection of the data set for the experiments was arbitrary, and all the experiments conducted on this data set can be also applied to other data sets in Ref. 16.

There are two reasons to select this data set. One is to demonstrate that the MPCM-PSSC has an application in chemical/biological defense. The other is to demonstrate that the MPCM-PSSC can be also used for ultraspectral signature characterization with thousands of spectral channels. Some other applications, such as hyperspectral laboratory data experiments, can be found in Ref. 17.

Example 1 (Spectral discrimination). In order to perform spectral discrimination using the MPCM-PSSC, we need to determine appropriate thresholds for each stage that are implemented by MPCM-PSSC stage by stage. For each signature we create a noise-corrupted signature with SNR 30 : 1, where the SNR was defined in Ref. 18 as the ratio of the 50%-reflectance signal to the noise standard deviation. Using the methyl salicylate signature in Fig. 5 as an example, the spectral signature is denoted by $\mathbf{r}$

Table 7 Spectral identification for a mixed signature, $\mathbf{s}=0.1\mathbf{s}_1+0.1\mathbf{s}_2+0.6\mathbf{t}+0.1\mathbf{s}_4+0.1\mathbf{s}_5$ with $\mathbf{t}=\mathbf{s}_3$.

Signature	1	2	3	4	5	6	7	8	9	10	11	12	13	SUM
$\mathbf{s}_1$	14	34	57	93	100	160	160	180	170	170	140	110	100	1488
$\mathbf{s}_2$	8	30	40	79	92	120	170	160	200	190	160	130	130	1509
$\mathbf{s}_3$	6	18	24	59	84	130	130	150	160	160	150	140	120	1331
$\mathbf{s}_4$	10	24	46	95	92	150	180	160	170	170	140	110	150	1497
$\mathbf{s}_5$	8	24	39	58	78	120	130	140	170	180	140	140	260	1487

Table 8 Spectral identification for a mixed signature, $\mathbf{s}=0.1\mathbf{s}_1+0.1\mathbf{s}_2+0.1\mathbf{s}_3+0.6\mathbf{t}+0.1\mathbf{s}_5$ with $\mathbf{t}=\mathbf{s}_4$.

Signature	1	2	3	4	5	6	7	8	9	10	11	12	13	SUM
$\mathbf{s}_1$	12	34	55	110	130	140	190	180	180	150	150	95	130	1556
$\mathbf{s}_2$	6	24	36	83	110	130	190	160	190	190	160	110	130	1519
$\mathbf{s}_3$	8	22	40	85	110	130	160	160	170	160	170	120	170	1505
$\mathbf{s}_4$	6	14	42	87	110	150	170	130	150	140	130	72	96	1297
$\mathbf{s}_5$	6	20	31	74	110	110	140	130	150	170	160	130	270	1501

$=(r_1,r_2,\ldots,r_{880})^T$. Then a noise-corrupted signature denoted by $\tilde{\mathbf{r}}=(\tilde{r}_1,\tilde{r}_2,\ldots,\tilde{r}_{880})^T$ can be obtained by adding a white Gaussian noise to each band to achieve a SNR of 30 : 1. Finally, the MPCM is applied to both the pure signature with no noise and the 30 : 1-SNR noise-corrupted signature to obtain their respective MPCM priority code words for band l, viz., $\mathbf{c}_l=(c_{l1},c_{l2},\ldots,c_{lM})^T$ and $\tilde{\mathbf{c}}_l=(\tilde{c}_{l1},\tilde{c}_{l2},\ldots,\tilde{c}_{lM})^T$ with $M=13$. Then the k'th stage threshold Δ_k is obtained by

$$\tau_k=\sum_{l=1}^{880} c_{lk}\oplus\tilde{c}_{lk}. \tag{12}$$

Table 3 tabulates all the stage thresholds $\{\tau_k\}_{k=1}^{M}$ for each of five signatures, methyl salicylate, pentanedione, propanoic acid, thiodiglycol, and heptanol, which are denoted by $\mathbf{s}_1$, $\mathbf{s}_2$, $\mathbf{s}_3$, $\mathbf{s}_4$, and $\mathbf{s}_5$.

It should be noted that the total number of stages, $M=13$, is determined by Eq. (6). As long as $\{\tau_k\}_{k=1}^{M}$ is determined, the discrimination process starts with the stage threshold in stage 1. If the distance between two signatures in stage 1 is greater than the threshold, the two signatures are declared to be distinct and discrimination process is terminated. Otherwise, the two signatures cannot be discriminated in stage 1, and the discrimination process is then passed on to stage 2, where the distance between the two signatures is calculated and compared with the threshold at stage 2. If the distance at stage 2 is greater than the threshold, the process is terminated. Otherwise, the same procedure is repeated until the last stage is reached.

Since the stage thresholds produced by one signature generally are different from those produced by another signature, the discrimination threshold is then determined by the minimum of the two different stage thresholds, that is, $\min\{\tau_i(\text{signature 1}),\ \tau_i(\text{signature 2})\}$. Table 4 shows the results where the stage thresholds in Table 3 were used for discrimination, and the shaded numbers are for the stages at which two signatures were discriminated. As we can see from Table 4, all the five signatures can be discriminated in stage 1.

Example 2 (Spectral identification). In this example, we further demonstrate the utility of the MPCM-PSSC in spectral identification via a database (spectral library) Γ, which consists of the five signatures in Fig. 9. For each target signature $\mathbf{t}$, 60% abundance fraction was simulated, the other four signatures sharing the remaining 40% abundance fraction at 10% each. Five different admixtures were generated by a fixed mixing composition (0.6, 0.1, 0.1, 0.1, 0.1) of the five signatures. When one of $\mathbf{s}_1$, $\mathbf{s}_2$, $\mathbf{s}_3$, $\mathbf{s}_4$, and $\mathbf{s}_5$ was designated as a target signature, say $\mathbf{s}_1$, a mixed signature $\mathbf{s}$ was then generated by mixing 0.6 of $\mathbf{s}_1$ with abundance fraction of 0.1 from each of the other four signatures $\mathbf{s}_2$, $\mathbf{s}_3$, $\mathbf{s}_4$, and $\mathbf{s}_5$. Table 5 tabulates a progressive spectral identification process for such a mixed signature $\mathbf{s}$, where $\mathbf{s}$ was quickly identified correctly by the target signature $\mathbf{t}=\mathbf{s}_1$ immediately by algorithm 1 in the first stage, as well as by algorithm 2.

Similar experiments were also performed by changing the designated target signature $\mathbf{t}$ from $\mathbf{s}_1$ to $\mathbf{s}_2$, $\mathbf{s}_3$, $\mathbf{s}_4$, and $\mathbf{s}_5$ for two spectral identification algorithms. Tables 6–9 tabulate their respective spectral progressive identification results. All the four mixed signatures are correctly identified by both algorithm 1 and algorithm 2. This experiment indicated that $\mathbf{s}_4$ as $\mathbf{s}_5$ are very similar to each other in spectral variation. Algorithm 1 had difficulty with identification until stage 2.

As a concluding remark, the abundance fraction of the target signature $\mathbf{t}$ has an effect on the performance of the MPCM-PSSC in identification. If the abundance fraction was greater than 60%, its performance improved significantly. Otherwise, its performance deteriorated as the abundance fraction diminished. In the following real image experiments, we further demonstrate that the MPCM-PSSC can still perform effectively when the estimated abundance fraction of a subpixel target is above 40%.

5 Real-Image Hyperspectral Experiments

The second data set used for experiments was a real image, shown in Fig. 10(a), from the HYperspectral Digital Imagery Collection Experiment (HYDICE). It has a size of 64 $\times$64 pixel vectors with 15 panels in the scene. Within the scene there is also a large grass field background, a forest on the left edge, and a barely visible road running on the right edge. Low-signal, high-noise bands (bands 1 to 3 and bands 202 to 210) and water vapor absorption bands (bands

Table 9 Spectral identification for a mixed signature, $\mathbf{s}=0.1\mathbf{s}_1+0.1\mathbf{s}_2+0.1\mathbf{s}_3+0.1\mathbf{s}_4+0.6\mathbf{t}$ with $\mathbf{t}=\mathbf{s}_5$.

Signature	1	2	3	4	5	6	7	8	9	10	11	12	13	SUM
$\mathbf{s}_1$	10	26	54	72	120	150	180	170	190	160	160	120	140	1552
$\mathbf{s}_2$	4	20	35	56	92	130	180	160	180	210	170	130	170	1537
$\mathbf{s}_3$	6	16	41	58	94	120	150	160	180	170	170	150	160	1475
$\mathbf{s}_4$	6	16	47	72	94	150	190	140	170	160	150	98	170	1463
$\mathbf{s}_5$	2	6	28	37	88	110	130	130	150	150	150	130	230	1341

101 to 112 and bands 137 to 153) were removed. The spatial resolution is 1.56 m, and the spectral resolution is 10 nm. There are 15 panels located in the center of the grass field and arranged in a 5×3 matrix as shown in Fig. 10(b), which provides the ground truth map of Fig. 10(a). Each element in this matrix is a square panel and denoted by p_{ij} with row indexed by $i=1,2,3,4,5$ and column indexed by $j=1,2,3$. For each row, the three panels p_{i1}, p_{i2}, p_{i3} were painted with the same material but have three different sizes. For each column $j=1,2,3$, the five panels p_{1j}, p_{2j}, p_{3j}, p_{4j}, p_{5j} have the same size but were painted with five different materials. It should be noted that the panels in rows 2 and 3 are made of the same material, but with different paints; likewise the panels in rows 4 and 5. Nevertheless, they were still considered as different materials. The sizes of the panels in the first, second, and third columns are 3×3, 2×2, and 1×1 m, respectively. So the 15 panels have five different materials and three different sizes. Figure 10(b) shows the precise spatial locations of these 15 panels, where red (R;) pixels are the panel center pixels, and yellow (Y) pixels are panel pixels mixed with background. The 1.56-m spatial resolution of the image scene suggests that most of the 15 panels are one pixel in size except for p_{21}, p_{31}, p_{41}, p_{51}, which are two-pixel panels, their pixels being denoted by p_{211}, p_{221}, p_{311}, p_{312}, p_{411}, p_{412}, p_{511}, p_{521}. Since the size of the panels in the third column is 1×1 m, they cannot be seen visually in Fig. 10(a), because their size is less than the 1.56-m pixel resolution.

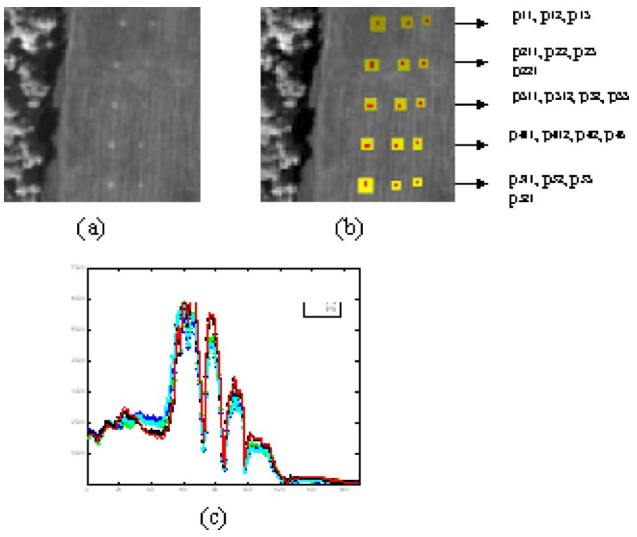

Fig. 10 (a) A HYDICE panel scene that contains 15 panels; (b) ground truth map of spatial locations of the 15 panels; (c) spectral signatures of panels $\mathbf{p}_1$, $\mathbf{p}_2$, $\mathbf{p}_3$, $\mathbf{p}_4$, and $\mathbf{p}_5$. x-coordinates: band numbers; y-coordinates: priority code words.

Figure 10(c) plots the five panel spectral signatures $\{p_i\}_{i=1}^5$ obtained from Fig. 10(b), where the i'th panel signature, p_i, was generated by averaging the R pixels in row i. These panel signature are used to represent target knowledge of the panels in each row.

Two scenarios have been conducted for experiments based on this 15-panel HYDICE scene. One is spectral discrimination among the five panel signatures, p_1, p_2, p_3, p_4, and p_5. The other is identifying the 15 panels unsupervised, using only knowledge obtained directly from the data.

Example 3 (Spectral discrimination). As in example 1, the spectral discrimination was performed by the MPCM-PSSC, for which number of stages required was calculated by Eq. (6) to be $M=13$ and the stage levels $\{\Delta_k\}_{k=1}^{13}$ were obtained by Eq. (7). In order to implement MPCM-PSSC algorithms, we also need to determine an appropriate set of stage thresholds.

In the same way as in example 1, the desired set of stage thresholds $\{\tau_k\}_{k=1}^{13}$ (Table 10) were obtained by Eq. (13), using noise-corrupted signatures with SNR set to 30:1 as a variation of the signature tolerance.

Table 11 tabulates the discrimination results obtained by the MPCM-PSSC among the five panel signatures $\{p_i\}_{i=1}^5$ in Fig. 10(c). As shown in Table 11, p_1 and p_2 are more similar to each other than to the other three panel signatures, since the discrimination could be accomplished in stage 2 in terms of spectral variation, in contrast with the other signature discrimination, which was made in stage 1.

Example 4 (Spectral identification). The experiments conducted in this example are very interesting and offer several intriguing results and observations. It was designed to identify the 19 (R) panel pixels, $\mathbf{p}_{ij}$ in Fig. 10(b) by the MPCM-PSSC. Since the panel pixels p_{13}, p_{23}, p_{33}, p_{43}, p_{53} have size 1×1 m, which is smaller than the pixel size, their abundance fractions present in single pixels can be at most $1/(1.56)^2=0.4109$, which can be interpreted as approximately 50% of the pixel size. As a result, the perfor-

Table 10 Stage thresholds for five panel signatures with SNR 30 : 1.

Panel	1	2	3	4	5	6	7	8	9	10	11	12	13
$\mathbf{p}_1$	2	1	5	10	14	24	23	16	16	16	9	4	4
$\mathbf{p}_2$	2	2	14	9	13	23	24	15	13	11	10	4	4
$\mathbf{p}_3$	1	4	6	8	16	19	21	13	11	11	7	6	5
$\mathbf{p}_4$	3	6	3	11	15	21	23	20	16	12	7	7	3
$\mathbf{p}_5$	3	6	4	10	16	19	21	18	13	10	7	4	3

mance in identification of these subpixel panels can be expected to be very challenging and difficult. On the other hand, due to its very high spatial and spectral resolution, the spectral variations of image pixels in this HYDICE scene can be very subtle and sensitive. Therefore, using the five panel signatures $\{p_i\}_{i=1}^5$ in Fig. 10(c) as a database may not be appropriate. Instead, a more effective database must be obtained in an unsupervised way, directly from data. In doing so, the result of the 34 target pixels generated directly from the scene by an unsupervised fully constrained least-squares (UFCLS) method developed in Refs. 11 and 19 was used to form a desired database Γ. Among these 34 generated target pixels there were five panel pixels identified as corresponding to the five distinct panel signatures $\{p_i\}_{i=1}^5$. Table 12 tabulates the results produced by the MPCM-PSSC using Algorithm 1 and Algorithm 2 for target identification along with the abundance fractions of the 19 R pixels estimated by the fully constrained least-squares method in Ref. 19, where an identification error is highlighted by shading.

According to Table 12, Algorithm 1 yielded the best performance in the sense that it only missed identification of the panels, p_{13}, p_{212}, p_{33}, p_{412}, p_{43}, p_{53} with estimated abundance fractions less than 0.3821. Algorithm 2 also made six identification errors, but it seemed that these misidentifications had no clear tie to the abundance fractions as with Algorithm 1. For example, it correctly identified p_{212}, whose abundance is only 0.3141, but it misidentified p_{32}, whose abundance is 0.5343. Compared to Algorithm 2, the SAM and the spectral information divergence (SID)[11,12] not only made the same six identification errors as did Algorithm 2, but also made two additional errors, which are panel pixels p_{511}, p_{52} with abundance fractions 0.7203 and 0.7789.

This experiment showed that the MPCM-PSSC performed more effectively than a pixel-based spectral similarity measure such as SAM and SID in Table 12. It should be noted that real target pixels in Table 12 were compared against the five panel signatures $\{p_i\}_{i=1}^5$ for analysis.

It is interesting to note that when the five panel signatures $\{p_i\}_{i=1}^5$ in Fig. 10(c) were directly used for identification, the results were reported in Ref. 17 and were not as good as the results in Table 12 that were produced by using the real target pixels in Table 12. This is primarily because

Table 11 Discrimination among five panel signatures using the stage thresholds in Table 10.

Panels	1	2	3	4	5	6	7	8	9	10	11	12	13
$\mathbf{p}_1$-$\mathbf{p}_2$	2	2	10	13	20	32	30	24	29	21	16	4	5
$\mathbf{p}_1$-$\mathbf{p}_3$	4	4	17	23	28	29	31	26	24	22	11	6	5
$\mathbf{p}_1$-$\mathbf{p}_4$	4	8	8	22	26	37	32	26	22	23	10	6	4
$\mathbf{p}_1$-$\mathbf{p}_5$	4	8	11	22	32	34	34	21	13	16	12	2	5
$\mathbf{p}_2$-$\mathbf{p}_3$	2	2	13	12	24	35	31	22	21	9	11	6	4
$\mathbf{p}_2$-$\mathbf{p}_4$	4	8	14	23	28	33	36	22	21	10	10	8	3
$\mathbf{p}_2$-$\mathbf{p}_5$	4	8	17	23	28	30	30	25	28	13	8	4	4
$\mathbf{p}_3$-$\mathbf{p}_4$	6	10	19	27	30	34	31	12	20	13	9	10	5
$\mathbf{p}_3$-$\mathbf{p}_5$	6	10	22	29	34	35	29	29	17	16	7	6	6
$\mathbf{p}_4$-$\mathbf{p}_5$	4	8	3	6	16	25	24	29	21	13	4	6	1

Table 12 Identification of 19 R panel pixels in Fig. 10(a).

Panel pixels	Algorithm 1	Algorithm 2	SAM/ SID	Abundance fractions estimated by FCLS
p_{11}	$\mathbf{p}_1$	$\mathbf{p}_1$	$\mathbf{p}_1$	1
p_{12}	$\mathbf{p}_1$	$\mathbf{p}_2$	$\mathbf{p}_2$	0.4098
p_{13}	$\mathbf{p}_3$	$\mathbf{p}_2$	$\mathbf{p}_2$	0.0499
p_{211}	$\mathbf{p}_2$	$\mathbf{p}_2$	$\mathbf{p}_2$	0.5255
p_{221}	$\mathbf{p}_3$	$\mathbf{p}_2$	$\mathbf{p}_2$	0.3141
p_{22}	$\mathbf{p}_2$	$\mathbf{p}_2$	$\mathbf{p}_2$	0.6917
p_{23}	$\mathbf{p}_2$	$\mathbf{p}_2$	$\mathbf{p}_2$	0.4221
p_{311}	$\mathbf{p}_3$	$\mathbf{p}_3$	$\mathbf{p}_3$	0.8647
p_{312}	$\mathbf{p}_3$	$\mathbf{p}_3$	$\mathbf{p}_3$	1
p_{32}	$\mathbf{p}_3$	$\mathbf{p}_2$	$\mathbf{p}_2$	0.5343
p_{33}	$\mathbf{p}_2$	$\mathbf{p}_2$	$\mathbf{p}_2$	0.3285
p_{411}	$\mathbf{p}_4$	$\mathbf{p}_4$	$\mathbf{p}_4$	1
p_{412}	$\mathbf{p}_5$	$\mathbf{p}_4$	$\mathbf{p}_4$	0.3821
p_{42}	$\mathbf{p}_4$	$\mathbf{p}_4$	$\mathbf{p}_4$	0.7034
p_{43}	$\mathbf{p}_2$	$\mathbf{p}_2$	$\mathbf{p}_2$	0.2242
p_{511}	$\mathbf{p}_5$	$\mathbf{p}_5$	$\mathbf{p}_4$	0.7203
p_{521}	$\mathbf{p}_5$	$\mathbf{p}_5$	$\mathbf{p}_5$	1
p_{52}	$\mathbf{p}_5$	$\mathbf{p}_5$	$\mathbf{p}_4$	0.7789
p_{53}	$\mathbf{p}_2$	$\mathbf{p}_2$	$\mathbf{p}_2$	0.1466

the signatures $\{p_i\}_{i=1}^{5}$ obtained by averaging R-panel pixels are not real pixels, but rather signatures. As a result, the signature variations of real target pixels have been compromised. The MPCM-PSSC seemed to remedy such deficiency by capturing subtle spectral variations in multiple stages, which can dictate changes in subtle difference encountered in real data as shown in Table 12.

As a final comment, it should be noted that the 34 target pixels used in this experiment were shown in Ref. 19 to be sufficient to include target pixels that represent the five distinct panel spectral signatures. However, that did not imply that it required at least 34 target pixels to do so. There may be some unsupervised target detection and classification algorithms that can generate fewer target pixels than 34 but still include pixels that can represent all the desired five panel signatures. In that case, these generated target pixels can be used as a database as well. As expected, the conclusion drawn from Table 12 will remain unchanged.

6 Conclusions

This paper introduces a new concept of progressive spectral signature coding (PSSC) for hyperspectral signature characterization. It is derived from a technique called multistage pulse code modulation (MPCM), which was previously developed for progressive image reconstruction and edge detection. Unlike the commonly used spectral signature coding, which performs coding with hard decisions, the proposed PSSC characterizes a hyperspectral signature in a sequence of soft decisions in multiple stages to produce a profile of progressive changes in spectral variation of the spectral signature. The idea of the MPCM-based PSSC (MPCM-PSSC) is to use a sequence of soft-decision-based quantizers to generate a priority code for a hyperspectral signature, which can be used to prioritize the signature values across its spectral coverage according to priorities specified by stage levels implemented in various stages. Such a priority code allows one to decompose and reconstruct a hyperspectral signature progressively in accordance with the priorities assigned to spectral signature values in wavelengths. As a result, a profile of progressive changes in spectral variation can be generated for a hyperspectral signature and can be further used to dictate subtle differences in spectral characterization. In order to substantiate the utility of the proposed MPCM-PSSC, applications in spectral discrimination and identification have been considered and investigated. Experiments have also been conducted to demonstrate unique features of the MPCM-PSSC in hyperspectral signature characterization, such as progressive spectral changes, progressive signature decomposition, and progressive signature reconstruction, which cannot be found in any spectral signature coding.

Acknowledgments

The first author would like to acknowledge support received from his NRC (National Research Council) senior research associateship sponsored by the U.S. Army Soldier and Biological Command, Edgewood Chemical and Biological Center (ECBC) from 2002–2003.

References

1. K. H. Tzou, "Progressive image transmission: a review and comparison of techniques," *Opt. Eng.* **26**(7), 581–589 (1987).
2. L. Wang and M. Goldberg, "Progressive image transmission using vector quantization on images in pyramid form," *IEEE Trans. Commun.* **37**(12), 1339–1349 (1989).
3. L. Wang and M. Goldberg, "Progressive image transmission by transform coefficient residual error quantization," *IEEE Trans. Commun.* **36**(1), 75–87 (1988).
4. Y. Cheng, "Multistage pulse code modulation (MPCM)," MS Thesis, Dept. of Electrical Engineering, Univ. of Maryland, Baltimore County; Baltimore (1993).
5. C.-I Chang, Y. Cheng, M. L. G. Althouse, L. Zhang, and J. Wang, "Multistage image coding: a top-down gray-level triangle method," in *Proc. Int. Symp. on Spectral Sensing Research (ISSSR)*, pp. 497–511 (1992).
6. C.-I Chang, Y. Cheng, and M. L. G. Althouse, "Chemical vapor detection using multistage predictive coding," in *Proc. Scientific Conf. on Chemical Defense Research*, pp. 909–915 CRDEC (1992).
7. C.-J. Chang, C.-I Chang, and M.-L. Chang, "Subband multistage predictive coding," *Proc. Int. Conf. on Signal Processing '93/Beijing*, pp. 783–787 (1993).
8. C.-I Chang, Y. Cheng, J. Wang, M. L. G. Althouse, and M. L. Chang, "Progressive edge extraction using multistage predictive coding," *Proc. 1994 Int. Symp. on Speech, Image and Neural Networks*, pp. 57–60 (1994).
9. Y. Du, C.-I Chang, and P. Thouin, "An automatic system for text detection in single video images," *J. Electron. Imaging* **12**(3), 410–422 (2003).
10. R. A. Schwengerdt, *Remote Sensing, Models and Methods for Image Processing*, 2nd ed., New York, Academic Press (1997).
11. C.-I Chang, *Hyperspectral Imaging: Techniques for Spectral Detection and Classification*, Kluwer Academic/Plenum Publishers (2003).

12. C.-I Chang, "An information theoretic-based approach to spectral variability, similarity and discriminability for hyperspectral image analysis," *IEEE Trans. Inf. Theory* **46**(5), 1927–1932 (2000).
13. A. Gersho and R. M. Gray, *Vector Quantization and Signal Compression*, Kluwer Academic Publishers (1992).
14. B. H. Juang and A. H. Gray, Jr., "Multiple stage vector quantization for speech coding," in *Proc. IEEE Conf. on ASSP*, Vol. **1**, pp. 597–600 (1982).
15. S. Mallat, "A theory for multiresolution signal decomposition," *IEEE Trans. Pattern Anal. Mach. Intell.* **11**(7), 674–693 (1989).
16. webbook.nist.gov/chemistry.
17. C.-I Chang, J. Wang, F. D'Amico, and J. O. Jensen, "Multistage pulse code modulation for progressive spectral signature coding," in *Chemical and Biological Standoff Detection II*, *Proc. SPIE* **5584**, 252–261 (2003).
18. J. Harsanyi and C.-I Chang, "Hyperspectral image classification and dimensionality reduction: an orthogonal subspace projection approach," *IEEE Trans. Geosci. Remote Sens.* **32**(4), 779–785 (1994).
19. D. Heinz and C.-I Chang, (2001), "Fully constrained least squares linear mixture analysis for material quantification in hyperspectral imagery," *IEEE Trans. Geosci. Remote Sens.* **39**(3), 529–545 (2001).

Chein-I Chang received his BS degree from Soochow University, Taipei, Taiwan, his MS degree from the Institute of Mathematics at National Tsing Hua University, Hsinchu, Taiwan, and his MA degree from the State University of New York at Stony Brook, all in mathematics. He also received his MS and MSEE degrees from the University of Illinois at Urbana-Champaign and his PhD degree in electrical engineering from the University of Maryland, College Park. He has been with the University of Maryland, Baltimore County (UMBC) since 1987 and is currently a professor in the Department of Computer Science and Electrical Engineering. He was a distinguished lecturer chair at the National Chung Hsing University, sponsored by the Ministry of Education in Taiwan from 2005 to 2006 and is currently holding a chair professorship with National Chung Hsing University. He has three patents and several pending on hyperspectral image processing. He is on the editorial board of the *Journal of High Speed Networks* and was the guest editor of a special issue of the same journal on telemedicine and applications and will co-edit two special issues on Broadband Multimedia Sensor Networks in Healthcare Applications for *Journal of High Speed Networks* and on High Performance Computing of Hyperspectral Imaging for *International Journal of High Performance Computing Applications*, . His research interests include multispectral/hyperspectral image processing, automatic target recognition, medical imaging, information theory and coding, signal detection and estimation, and neural networks.

Jing Wang received her BS degree in electrical engineering and the MS degree in computer engineering from the Beijing University of Post and Telecommunications in 1998 and 2001. She also received her PhD degree in electrical engineering from the University of Maryland, Baltimore County (UMBC), Baltimore, in 2006. Currently she is a research member of Xerox Wilson Center for Research and Technology (WCR&T) in Webster, NY.

Chein-Chi Chang received his BS degree from Tamkang University, Taiwan, in 1979; his MS degree from the Ohio State University in 1981; and his PhD degree in civil engineering from the University of Missouri–Rolla in 1988. He has been a senior engineer with District of Columbia Water and Sewer Authority since 2000. Before his current position, he had worked with numerous engineering consulting companies. He has been an adjunct professor at four universities: University of Maryland, Baltimore County; University of Northern Virginia; China Hunan University; and China Central South University. He has been in several engineering societies: the American Society of Civil Engineers, the Chinese Institute of Engineers—USA, and the Overseas Chinese Environmental Engineers and Scientists Association. His research interests include multispectral/hyperspectral image processing in environmental applications, system optimizations, remote sensing, geographic information systems, and water resources engineering.

Chinsu Lin received his MS and PhD degrees in forestry from National Taiwan University in 1988 and 1996, respectively. He is currently a full professor and the head of the Department of Forestry and Natural Resources at National Chiayi University (NCYU), Taiwan. His research interests include multispectral and hyperspectral signal processing and pattern recognition. He is currently investigating applications of remote sensing techniques in extraction of spatial information for forest ecosystem management; the major applications are automatic delineation and mapping of individual tree canopy, forest biomass and productivity, carbon fixation estimation, individual-based tree species classification, and wireless sensor networks for monitoring the ecosystem environment. He also makes efforts at upgrading the forest inventory accuracy by incorporating the techniques of hyperspectral and hyperspatial remote sensing, GIS, and GPS.